Progress In Electromagnetics Research, Vol. 126, 375–398, 2012

HYBRID TDIE-TDPO METHOD USING WEIGHTED LAGUERRE POLYNOMIALS FOR SOLVING TRANSIENT ELECTROMAGNETIC PROBLEMS

M.-D. Zhu[1,*], X.-L. Zhou[1], W. Luo[1], and W.-Y. Yin[1,2]

[1]Center for Microwave and RF Technologies, Key Lab of Ministry of Education for Design and EMC of High Speed Electronic Systems, Shanghai Jiao Tong University, Shanghai 200240, China

[2]Center for Optical and EM Research (COER), State Key Lab of MOI Zhejiang University, Hangzhou 310058, China

Abstract—An efficient and stable hybrid method, based on the time-domain integral equation (TDIE) and time-domain physical optics (TDPO), is developed for investigating transient radiation and scattering from perfectly electrical conducting (PEC) objects. It at first requires partitioning the PEC object surface into TDIE and TDPO regions, respectively. Then, a set of hybrid TDIE-TDPO equations is derived and solved using an adaptive marching-on-in-degree (MOD) method. The fast Fourier transforms (FFT)-based blocking scheme is further implemented into the proposed algorithm so as to reduce N_O^2 dependence of the traditional MOD method to $N_O \log^2(N_O)$, where N_O is the highest order of the weighted Laguerre polynomials used for computation. Under such circumstances, its computational cost, in comparison with the full TDIE-MOD solver, is reduced significantly. Several numerical examples are presented to demonstrate its accuracy and efficiency in solving some typical transient electromagnetic problems.

1. INTRODUCTION

It is well known that wideband transient responses of conductive objects are often required in handling various electromagnetic compatibility (EMC) and electromagnetic interference (EMI) problems of complex platforms. Under such circumstances, the time-domain integral equation (TDIE) method [1–13, 34] is often used with

Received 13 November 2011, Accepted 27 December 2011, Scheduled 26 March 2012

* Corresponding author: Ming-Da Zhu (zhumda@sjtu.edu.cn).

marching-on-in-time (MOT) scheme implemented. However, MOT suffers from the occurrence of late time instabilities in the form of exponentially increasing oscillation. Therefore, many studies have been devoted to eliminating such instabilities. As indicated in [2–4], good stability for arbitrary structures and for any time step size can be obtained with an appropriate algorithm adopted.

Recently, a new method of marching-on-in-degree (MOD) has been proposed by some researchers [5–7]. It employs the weighted Laguerre polynomials as entire domain temporal basis and testing functions. MOD scheme has following properties: 1) A truncation error, instead of the temporal discretization error in MOT, is introduced in MOD implementation. The truncation error would not accumulate during the commutation; 2) It can completely eliminate temporal variables and interpolations; 3) The weighted Laguerre polynomials force the temporal solutions decaying exponentially. Therefore, stable transient electromagnetic responses can be obtained even for late time. However, such TDIE-MOD scheme, in general, results in dense linear systems, restricting its applicability when the number of unknowns is large.

On the other hand, we know that in order to handle an electrically large PEC object, time-domain physical optics (TDPO) [14, 35, 36] approximation is an appropriate choice. Nevertheless, these transient electromagnetic problems also involve locally small structures which cannot be handled accurately using the TDPO. One effective remedy is to employ hybridizations of both integral and optical methods in the time domain.

The idea of hybridizing current-based high frequency asymptotic technique, such as physical optics (PO), with the method of moments (MoM), has long been investigated. The approaches proposed in [15–19] treat smooth region of PEC objects with the PO method, and its remaining part by the MoM. On the other hand, several techniques have also been proposed for mirroring the frequency-domain current-based hybrid methods into the time domain, with an extension of hybridization as demonstrated in [20, 21] and MOT scheme implemented. However, in [20], only partial mutual interactions between the TDIE and TDPO regions are taken into account, while the effects of TDIE currents on TDPO ones are neglected. In [21], since the adopted hybrid formulation has the same computational complexity as that of conventional TDIE, plane-wave time-domain (PWTD) algorithm [11], which is highly technical for implementation, is required to accelerate the overall algorithm.

In this paper, an efficient hybrid TDIE-TDPO method with high stability, based on the weighted Laguerre polynomials and

MOD scheme, is proposed for investigating transient electromagnetic responses of 3-D composite PEC objects, while the TDPO approximation is applicable to the large PEC objects with smooth surface. These objects are partitioned into two regions: TDIE and TDPO ones. Such a hybrid TDIE-TDPO method has advantages over TDPO approximation alone, as it can control the approximation errors by changing the percentage of TDIE regions. On the other hand, since the proposed formulation is similar to its frequency-domain counterpart [15], the proposed method does not require any specific acceleration algorithm such as PWTD [21]. Its saving of both memory and CPU time is obtained by TDPO approximation. Therefore, the hybrid formula given in Section 2 can be directly applied for MOT scheme as well as finite difference delay modeling method [2] with no difficulty.

Here, the TDPO-TDPO projection part of the system matrix is made to be an identity block matrix by a projection procedure for the Rao–Wilton–Glisson (RWG) basis functions [24], while the original idea has been proposed for *PO*-MM method [15]. Thus, the reduction of dimension of system matrix can be obtained by this projection procedure. In other words, the reduced dimension of system matrix is equal to N_S^{IE} and irrespective of N_S^{PO}, where N_S^{IE} and N_S^{PO} is the number of spatial unknowns in TDIE and TDPO regions, respectively. Since the TDIE region is not electrically large for most hybrid problems, we can solve the linear equations by direct solver without convergence problem introduced by iterative methods. The method for adaptively determining the number of temporal basis functions and the fast Fourier transform (FFT)-based blocking scheme, similar as those given in [12, 13] for accelerating the temporal convolutions, is also employed.

2. FORMULATION

2.1. Time-domain Integral Equation

Figure 1 shows the geometry of some 3-D PEC objects consisting of arbitrary surfaces (S) and wires (W) located in an unbounded medium characterized by the permittivity ε and the permeability μ. The transient electric and magnetic fields $\{\vec{E}^i(\vec{r},t), \vec{H}^i(\vec{r},t)\}$ denote their excitation, and it can be an incident plane wave or a local voltage source along the wire segment. The line current $\vec{I}^{IE}$ along the wires and the surface current density $\vec{J}^{IE}$ on the surfaces are generated by the excitation. The transient scattered fields $\{\vec{E}^s(\vec{r},t), \vec{H}^s(\vec{r},t)\}$ can

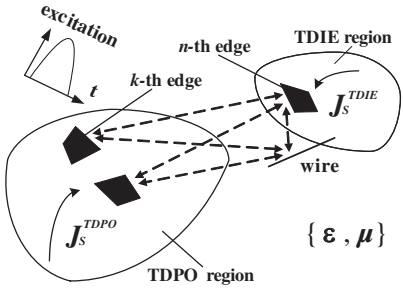

Figure 1. Subdivision of the 3-D PEC objects.

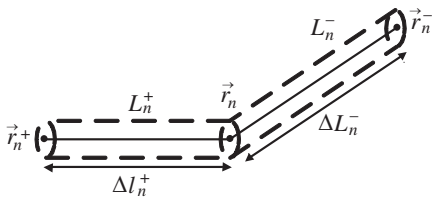

Figure 2. The geometry of a wire segment pair.

be expressed as

$$\vec{E}^s(\vec{r},t) = \vec{L}_S^E\left(\vec{J}^{IE}\right) + \vec{L}_W^E\left(\vec{I}^{IE}\right) \tag{1}$$

$$\vec{H}^s(\vec{r},t) = \vec{L}_S^H\left(\vec{J}^{IE}\right) + \vec{L}_W^H\left(\vec{I}^{IE}\right) \tag{2}$$

$$\vec{L}_S^E\left(\vec{J}^{IE}\right) = -\frac{\mu}{4\pi}\int_S \frac{1}{R}\frac{\partial}{\partial t}\vec{J}^{IE}(\vec{r},\tau)dS' + \frac{1}{4\pi\varepsilon}\nabla\int_S\int_0^\tau \frac{1}{R}\nabla'\cdot\vec{J}^{IE}(\vec{r},t)dtdS' \tag{3}$$

$$\vec{L}_W^E\left(\vec{I}^{IE}\right) = -\frac{\mu}{4\pi}\int_L\int_{-\pi}^{\pi}\frac{a}{R}\vec{I}^{IE}(\vec{r},\tau)d\varphi' dl' + \frac{1}{4\pi\varepsilon}\nabla\int_L\int_{-\pi}^{\pi}\int_0^\tau \frac{a}{R}\nabla' \cdot\vec{I}^{IE}(\vec{r},t)dtd\varphi' dl' \tag{4}$$

$$\vec{L}_S^H\left(\vec{J}^{IE}\right) = \frac{1}{4\pi}\nabla\times\int_S \frac{1}{R}\vec{J}^{IE}(\vec{r},\tau)\,dS' \tag{5}$$

$$\vec{L}_W^H\left(\vec{I}^{IE}\right) = \frac{1}{4\pi}\nabla\times\int_L\int_{-\pi}^{\pi}\frac{a}{R}\vec{I}^{IE}(\vec{r},\tau)\,d\varphi' dl' \tag{6}$$

where $R = |\vec{r} - \vec{r}'|$ represents the distance between an arbitrary observation point $\vec{r}$ and source point $\vec{r}'$, $\tau = t - R/c$ is the retarded time, c is the velocity of electromagnetic wave in the space, and a is the wire radius. Here, the wires are treated using a full-kernel expression [23].

We now divide the wires into N_W^{IE} segment pairs, as shown in Fig. 2. The segment pair $L_n^\pm$ is assigned to the element from $\vec{r}_n$ to $\vec{r}_n^\pm$. Then, we use a set of basis functions defined in [23] for the wire structure, and given by

$$\vec{f}_n^W(\vec{r}) = \begin{cases} \pm\dfrac{1}{2\pi a}\dfrac{\vec{l}_n^\pm}{\Delta l_n^\pm}, & \vec{r}\in L_n^\pm \\ 0, & \text{otherwise} \end{cases} \tag{7}$$

where $\Delta l_n^{\pm} = |\vec{r}_n - \vec{r}_n^{\pm}|$ is the length of the wire segment, and $\vec{l}_n^{\pm} = \vec{r} - \vec{r}_n^{\pm}$ is the local position vector.

When applying the MOD scheme, the temporal part of the unknown currents is approximated by a linear superposition of the orthogonal entire domain temporal basis functions [5], and written as

$$\phi_i(t) = e^{-t/2} L_i(t) \tag{8}$$

where $L_i(t)$ is the Laguerre polynomials of order i. Thus, the current densities $\vec{J}^{IE}$ and $\vec{I}^{IE}$ can be expanded as

$$\vec{J}^{IE}(\vec{r},t) = \sum_{n=1}^{N_S^{IE}} J_n^{IE}(t)\vec{f}_n^{S}(\vec{r}) = \sum_{n=1}^{N_S^{IE}} \left[\sum_{j=0}^{\infty} J_{n,j}^{IE}\phi_j(st)\right] \vec{f}_n^{S}(\vec{r}) \tag{9}$$

$$\vec{I}^{IE}(\vec{r},t) = \sum_{n=1}^{N_W^{IE}} I_n^{IE}(t)\vec{f}_n^{W}(\vec{r}) = \sum_{n=1}^{N_W^{IE}} \left[\sum_{j=0}^{\infty} I_{n,j}^{IE}\phi_j(st)\right] \vec{f}_n^{W}(\vec{r}) \tag{10}$$

where s is the scaling factor, $\vec{f}_n^{S}(\vec{r})$ is the RWG spatial basis function defined over triangular patches [24], and $\vec{f}_n^{W}(\vec{r})$ is the basis function defined by (7) for wire segments. Since the tangential components of the total electric field vanish on the PEC surface, we have

$$\left[\vec{E}^{s}(\vec{r},t) + \vec{E}^{i}(\vec{r},t)\right]_{\tan} = 0 \tag{11}$$

By inserting (9) and (10) into (11) and applying the adaptive MOD scheme [10], we can get the unknown coefficients by solving a set of matrix equations recursively.

2.2. Time-domain Hybridization

In Fig. 1, the PEC object surfaces are partitioned into TDIE and TDPO regions which are denoted by S^{IE} and S^{PO}, respectively. The determination of the percentage of TDIE regions is flexible, and it is based on the trade-off between accuracy and efficiency. The current densities $\vec{J}^{IE}$ and $\vec{I}^{IE}$ in the TDIE region are expanded according to (9) and (10). In the TDPO region, the surface current density $\vec{J}^{PO}$ is expanded as

$$\vec{J}^{PO}(\vec{r},t) = \sum_{k=1}^{N_S^{PO}} J_k^{PO}(t)\vec{f}_k^{S}(\vec{r}) = \sum_{k=1}^{N_S^{PO}} \left[\sum_{j=0}^{\infty} J_{k,j}^{PO}\phi_j(st)\right] \vec{f}_k^{S}(\vec{r}) \tag{12}$$

In contrast to the TDIE solution, the coefficients $J_{n,j}^{PO}$ are obtained through the TDPO approximation [14], and given by

$$\begin{aligned}\vec{J}^{PO}(\vec{r},t) &= \delta_{inc}\cdot 2\hat{n}\times\vec{H}^{i}(\vec{r},t)+\delta_{J,n}\cdot 2\hat{n}\times\vec{L}_{S}^{H}\left(\vec{J}^{IE}\right)\\ &\quad+\delta_{I,n}\cdot 2\hat{n}\times\vec{L}_{W}^{H}\left(\vec{I}^{IE}\right)\end{aligned}\tag{13}$$

where $\hat{n}$ denotes the outward pointing normal to S^{PO}, and δ_{inc} is the shadowing effect coefficient. If the point $\vec{r}$ lies in the shadowed region, δ_{inc} is zero, otherwise, it is unit one. The shadowing effects of point $\vec{r}$ in the TDPO region with respect to the current densities $\vec{J}^{IE}$ and $\vec{I}^{IE}$ are also included in (13) by the coefficients $\delta_{J,n}$ and $\delta_{I,n}$. For a simple convex object, δ_{inc} can be determined by a dot product between the direction of incident wave and each triangular facet normal. While for more complicated structures with shadow region involved, the shadowing techniques, such as the polygon ray tracer [25] and Z-buffer based methods [26, 27], is needed.

In [20], the TDPO current density is determined solely by local and time dependent magnetic field strength $\vec{H}^{i}(\vec{r},t)$. However, for transient radiation problems, it is confined surrounding the feeding in the TDIE region, i.e., $\vec{H}^{i}(\vec{r},t)$ is zero in the TDPO region. Therefore, the influence of currents in the TDIE region should be taken into account appropriately.

In order to avoid matrix inversion for obtaining the current expanding coefficients on the S^{PO}, a projection procedure which is similar to the *PO*-MM method [15], is adopted here. We use the notation k Two unit vectors $\hat{t}_k^{\pm}$ are introduced in the middle of the k-th edge, which are perpendicular to the k-th edge and lying in the plane of the triangles $T_k^{\pm}$. The vector $\vec{r}_k$ denotes the middle of the k-th edge. Therefore, with the *PO* projection procedure employed, the coefficients in the TDPO region are expressed as

$$J_k^{PO}(t)=\frac{1}{2}\left(\hat{t}_k^{+}+\hat{t}_k^{-}\right)\cdot\vec{J}^{PO}(\vec{r}_k,t)\tag{14}$$

Inserting (14) into (13) gives

$$\begin{aligned}J_k^{PO}(t)=&\left(\hat{t}_k^{+}+\hat{t}_k^{-}\right)\\ &\cdot\left[\delta_{inc}\cdot\hat{n}\times\vec{H}^{i}(\vec{r}_k,t)+\delta_{J,n}\cdot\hat{n}\times\vec{L}_{S}^{H}\left(\vec{J}^{IE}\right)+\delta_{I,n}v\cdot\hat{n}\times\vec{L}_{W}^{H}\left(\vec{I}^{IE}\right)\right]\end{aligned}\tag{15}$$

Applying the boundary condition (11) for the TDIE region leads to

$$\vec{E}^{i}(\vec{r},t)+\vec{L}_{S}^{E}\left(\vec{J}^{IE}\right)+\vec{L}_{W}^{E}\left(\vec{I}^{IE}\right)+\vec{L}_{S}^{E}\left(\vec{J}^{PO}\right)\Big|_{\tan}=0\tag{16}$$

In (16), the electric field radiated by the TDPO currents is taken into account, while the effects of currents in the TDIE region are included in (15).

2.3. Adaptive Mod Solution Method

2.3.1. Testing Procedure

A causal transient function $f(t)$ can be expanded as

$$f(t) = \sum_{j=0}^{\infty} f_j \phi_j(st) \tag{17}$$

with its integral and its first derivative given by [5]

$$\int_0^t f(\tau)\, d\tau = \frac{2}{s} \sum_{j=0}^{\infty} \left(f_j + 2 \sum_{l=0}^{j-1} (-1)^{j-l} f_l \right) \phi_j(st) \tag{18}$$

$$\frac{d}{dt} f(t) = s \sum_{j=0}^{\infty} \left(\frac{1}{2} f_j + \sum_{l=0}^{j-1} f_l \right) \phi_j(st) \tag{19}$$

where $f(0) = 0$ is assumed.

Substituting (5), (6), (9), (10) and (19) into (15), and using the weighted Laguerre polynomials $\phi_i(t)$ for the temporal Galerkin testing, we have

$$\begin{aligned} J_{k,i}^{PO} = V_{k,i}^{H} &+ \sum_{j=0}^{i} \sum_{n=1}^{N_S^{IE}} \frac{s}{4\pi c} \left(J_{n,j}^{IE} \right)^{(1)} \cdot a_{kn,i-j}^{1} + \sum_{j=0}^{i} \sum_{n=1}^{N_S^{IE}} \frac{1}{4\pi} J_{n,j}^{IE} \cdot a_{kn,i-j}^{2} \\ &+ \sum_{j=0}^{i} \sum_{n=1}^{N_W^{IE}} \frac{s}{4\pi c} \left(I_{n,j}^{IE} \right)^{(1)} \cdot b_{kn,i-j}^{1} + \sum_{j=0}^{i} \sum_{n=1}^{N_W^{IE}} \frac{1}{4\pi} I_{n,j}^{IE} \cdot b_{kn,i-j}^{2} \end{aligned} \tag{20}$$

with

$$a_{kn,i-j}^{1} = \delta_{J,n} \cdot \left(\hat{t}_k^{+} + \hat{t}_k^{-} \right) \cdot \hat{n} \times \int_S I_{ij} \left(\frac{sR}{c} \right) \vec{f}_n^{S}(\vec{r}\,') \times \frac{\hat{R}_k}{R_k} dS' \tag{21}$$

$$a_{kn,i-j}^{2} = \delta_{J,n} \cdot \left(\hat{t}_k^{+} + \hat{t}_k^{-} \right) \cdot \hat{n} \times \int_S I_{ij} \left(\frac{sR}{c} \right) \vec{f}_n^{S}(\vec{r}\,') \times \frac{\hat{R}_k}{R_k^2} dS' \tag{22}$$

$$b_{kn,i-j}^{1} = \delta_{I,n} \cdot \left(\hat{t}_k^{+} + \hat{t}_k^{-} \right) \cdot \hat{n} \times \int_L \int_{-\pi}^{\pi} I_{ij} \left(\frac{sR}{c} \right) \vec{f}_n^{W}(\vec{r}\,') \times \frac{\hat{R}_k}{R_k} a d\varphi' dl' \tag{23}$$

$$b^2_{kn,i-j}=\delta_{I,n}\cdot\left(\hat{t}^+_k+\hat{t}^-_k\right)\cdot\hat{n}\times\int_L\int_{-\pi}^{\pi}I_{ij}\left(\frac{sR}{c}\right)\vec{f}^W_n\left(\vec{r}\,'\right)\times\frac{\hat{R}_k}{R^2_k}ad\varphi' dl' \quad (24)$$

$$V^H_{k,i}=\delta_{I,n}\cdot\left(\hat{t}^+_k+\hat{t}^-_k\right)\cdot\int_0^{\infty}\phi_i\left(st\right)\cdot\hat{n}\times\vec{H}^i\left(\vec{r},t\right)d\left(st\right) \quad (25)$$

and

$$\begin{aligned}I_{ij}(sR/c) &= \int_{sR/c}^{\infty}\phi_i\left(st\right)\phi_j\left(st-sR/c\right)d\left(st\right)\\ &= \begin{cases}e^{-sR/(2c)}\left[L_{i-j}\left(sR/c\right)-L_{i-j-1}\left(sR/c\right)\right], & j<i\\ e^{-sR/(2c)}, & j=i,\\ o, & j>i\end{cases}\end{aligned} \quad (26)$$

$$\left(J^{IE}_{n,j}\right)^{(1)}=\frac{1}{2}J^{IE}_{n,j}+\sum_{l=0}^{j-1}J^{IE}_{n,l} \quad (27)$$

$$\left(I^{IE}_{n,j}\right)^{(1)}=\frac{1}{2}I^{IE}_{n,j}+\sum_{l=0}^{j-1}I^{IE}_{n,l} \quad (28)$$

where $R_k=|\vec{r}_k-\vec{r}\,'|$, and $\hat{R}_k$ is the unit vector along the direction $\vec{r}_k-\vec{r}\,'$.

Similarly, by inserting (3), (4), (9), (10), (12), (18) and (19) into (16), and applying the spatial and temporal Galerkin testing procedure, we obtain

$$\begin{aligned}&\sum_{j=0}^{i}\sum_{n=1}^{N^{IE}_S}\frac{\mu s}{4\pi}\left(J^{IE}_{n,j}\right)^{(1)}\cdot c^s_{mn,i-j}+\sum_{j=0}^{i}\sum_{n=1}^{N^{IE}_S}\frac{1}{2\pi\varepsilon s}\left(J^{IE}_{n,j}\right)^{(-1)}\cdot c^h_{mn,i-j}\\ &+\sum_{j=0}^{i}\sum_{n=1}^{N^{IE}_W}\frac{\mu s}{4\pi}\left(I^{IE}_{n,j}\right)^{(1)}\cdot d^s_{mn,i-j}+\sum_{j=0}^{i}\sum_{n=1}^{N^{IE}_W}\frac{1}{2\pi\varepsilon s}\left(I^{IE}_{n,j}\right)^{(-1)}\cdot d^h_{mn,i-j}\\ &+\sum_{j=0}^{i}\sum_{k=1}^{N^{PO}_S}\frac{\mu s}{4\pi}\left(J^{PO}_{k,j}\right)^{(1)}\cdot c^s_{mk,i-j}+\sum_{j=0}^{i}\sum_{k=1}^{N^{PO}_S}\frac{1}{2\pi\varepsilon s}\left(J^{PO}_{k,j}\right)^{(-1)}\cdot c^h_{mk,i-j}=V^E_{m,i}\end{aligned} \quad (29)$$

$$\begin{aligned}&\sum_{j=0}^{i}\sum_{n=1}^{N^{IE}_S}\frac{\mu s}{4\pi}\left(J^{IE}_{n,j}\right)^{(1)}\cdot e^s_{mn,i-j}+\sum_{j=0}^{i}\sum_{n=1}^{N^{IE}_S}\frac{1}{2\pi\varepsilon s}\left(J^{IE}_{n,j}\right)^{(-1)}\cdot e^h_{mn,i-j}\\ &+\sum_{j=0}^{i}\sum_{n=1}^{N^{IE}_W}\frac{\mu s}{4\pi}\left(I^{IE}_{n,j}\right)^{(1)}\cdot f^s_{mn,i-j}+\sum_{j=0}^{i}\sum_{n=1}^{N^{IE}_W}\frac{1}{2\pi\varepsilon s}\left(I^{IE}_{n,j}\right)^{(-1)}\cdot f^h_{mn,i-j}\end{aligned}$$

$$+\sum_{j=0}^{i}\sum_{k=1}^{N_S^{PO}}\frac{\mu s}{4\pi}\left(J_{k,j}^{PO}\right)^{(1)}\cdot e_{mk,i-j}^{s}+\sum_{j=0}^{i}\sum_{k=1}^{N_S^{PO}}\frac{1}{2\pi\varepsilon s}\left(J_{k,j}^{PO}\right)^{(-1)}\cdot e_{mk,i-j}^{h}=U_{m,i}^{E} \quad (30)$$

with

$$V_{m,i}^{E} = \int_S \vec{f}_m^{S}(\vec{r})\cdot\int_0^{\infty}\phi_i(st)\vec{E}^{\,i}(\vec{r},t)\,d(st)\,dS \quad (31)$$

$$U_{m,i}^{E} = \int_L\int_{-\pi}^{\pi}\vec{f}_m^{W}(\vec{r})\cdot\int_0^{\infty}\phi_i(st)\vec{E}^{\,i}(\vec{r},t)\,d(st)\,ad\varphi dl \quad (32)$$

$$\left(J_{k,j}^{PO}\right)^{(1)} = \frac{1}{2}J_{k,j}^{PO}+\sum_{l=0}^{j-1}J_{k,l}^{PO} \quad (33)$$

$$\left(J_{k,j}^{PO}\right)^{(-1)} = J_{k,j}^{PO}+2\sum_{l=0}^{j-1}(-1)^{j-l}J_{k,l}^{PO} \quad (34)$$

$$\left(J_{n,j}^{IE}\right)^{(-1)} = J_{n,j}^{IE}+2\sum_{l=0}^{j-1}(-1)^{j-l}J_{n,l}^{IE} \quad (35)$$

$$\left(I_{n,j}^{IE}\right)^{(-1)} = I_{n,j}^{IE}+2\sum_{l=0}^{j-1}(-1)^{j-l}I_{n,l}^{IE} \quad (36)$$

where the variables in (29) and (30) are given in Appendix A, and they are the matrix equations for the TDIE region. However, the linear Equations (20), (29) and (30) are a set of coupled equations and they are not solvable yet, because of the unknown coefficients existing in both TDIE and TDPO regions for current order i. Thus, by inserting (20) into (29) and (30), we obtain

$$\begin{aligned}
&\sum_{n=1}^{N_S^{IE}}Z_{mn}^{SS}J_{n,i}^{IE}+\sum_{n=1}^{N_W^{IE}}Z_{mn}^{SW}I_{n,i}^{IE}=V_{m,i}^{E}-P_{m,i}^{IE}-P_{m,i}^{PO}-\sum_{k=1}^{N_S^{PO}}\beta_{mk}^{SS}V_{k,i}^{H}\\
&-\sum_{k=1}^{N_S^{PO}}\beta_{mk}^{SS}\frac{s}{4\pi c}\left[\sum_{n=1}^{N_S^{IE}}a_{kn,0}^{1}\sum_{l=0}^{i-1}J_{n,l}^{IE}+\sum_{n=1}^{N_W^{IE}}b_{kn,0}^{1}\sum_{l=0}^{i-1}I_{n,l}^{IE}\right]\\
&-\sum_{k=1}^{N_S^{PO}}\beta_{mk}^{SS}\sum_{j=0}^{i-1}\left\{\sum_{n=1}^{N_S^{IE}}\left[\frac{s}{4\pi c}a_{kn,i-j}^{1}\left(J_{n,j}^{IE}\right)^{(1)}+\frac{1}{4\pi}a_{kn,i-j}^{2}J_{n,j}^{IE}\right]\right.\\
&\left.+\sum_{n=1}^{N_W^{IE}}\left[\frac{s}{4\pi c}b_{kn,i-j}^{1}\left(I_{n,j}^{IE}\right)^{(1)}+\frac{1}{4\pi}b_{kn,i-j}^{2}I_{n,j}^{IE}\right]\right\}
\end{aligned} \quad (37)$$

$$\sum_{n=1}^{N_S^{IE}} Z_{mn}^{WS} J_{n,i}^{IE} + \sum_{n=1}^{N_W^{IE}} Z_{mn}^{WW} I_{n,i}^{IE} = U_{m,i}^{E} - Q_{m,i}^{IE} - Q_{m,i}^{PO} - \sum_{k=1}^{N_S^{PO}} \beta_{mk}^{WS} V_{k,i}^{H}$$
$$- \sum_{k=1}^{N_S^{PO}} \beta_{mk}^{WS} \frac{s}{4\pi c} \left[\sum_{n=1}^{N_S^{IE}} a_{kn,0}^{1} \sum_{l=0}^{i-1} J_{n,l}^{IE} + \sum_{n=1}^{N_W^{IE}} b_{kn,0}^{1} \sum_{l=0}^{i-1} I_{n,l}^{IE} \right]$$
$$- \sum_{k=1}^{N_S^{PO}} \beta_{mk}^{WS} \sum_{j=0}^{i-1} \left\{ \sum_{n=1}^{N_S^{IE}} \left[\frac{s}{4\pi c} a_{kn,i-j}^{1} \left(J_{n,j}^{IE} \right)^{(1)} + \frac{1}{4\pi} a_{kn,i-j}^{2} J_{n,j}^{IE} \right] \right.$$
$$\left. + \sum_{n=1}^{N_W^{IE}} \left[\frac{s}{4\pi c} b_{kn,i-j}^{1} \left(I_{n,j}^{IE} \right)^{(1)} + \frac{1}{4\pi} b_{kn,i-j}^{2} I_{n,j}^{IE} \right] \right\} \tag{38}$$

where the variables in (37) and (38) are also given in Appendix A. Both (37) and (38) are solved firstly so as to get the unknown coefficients $J_{n,i}^{IE}$ and $I_{n,i}^{IE}$ in the TDIE regions for current order i, and they are solved once for each order. When $J_{n,i}^{IE}$ and $I_{n,i}^{IE}$ are obtained, (20) can be further solved so as to get the unknown coefficients $J_{n,i}^{PO}$ in the TDPO regions for current order i. As all unknown coefficients for order i are obtained, the algorithm is marching on to the next order $i+1$.

Therefore, we can solve the TDIE-TDPO hybrid formula (15) and (16) in the MOD manner. Since the geometries of objects and TDPO approximations only affect the temporal waveforms of TDIE and TDPO currents rather than the existence and uniqueness of the solution of hybrid TDIE-TDPO method, the convergence and stability properties of MOD scheme are not changed. Its accuracy and efficiency depends on:

a) the spatial unknown numbers $N_S^{IE} + N_W^{IE}$ and N_S^{PO};
b) the scaling factor s;
c) the highest order N_O of the weighted Laguerre polynomials used for computation.

If the transient signal is frequency-limited to W, where $-50\,\mathrm{dB}$ is reached, we choose an appropriate scaling factor as $s = 4\pi W$. According to the known incident wave and the stopping criterion in Sections 2.3.3 and 2.3.4, we can also check and justify the scaling factor before computation.

2.3.2. Acceleration of Temporal Convolution by FFT

If we directly apply the above hybrid method for solving transient scattering and radiation problems, it will suffer from N_O^2 dependence of the MOD scheme. Therefore, the blocking technique proposed in [28], which does not disturb the marching-on-in-degree nature, is adopted so as to accelerate temporal convolutions on the right-hand side of (20), (37) and (38).

Since the MOD kernel $I_{ij}(sR/c)$ does not have any explicit form and it is computed recursively, evaluating the matrix elements separately ruins the acceleration of temporal convolutions by FFT. For example, at order 4, the matrix elements of $[a^1_{kn,i}]$, $i = 1, 2, \ldots,$ and 7, at row m and column n are arranged in the vector form of

$$\left[a^1_{kn,4}, a^1_{kn,5}, a^1_{kn,6}, a^1_{kn,7}, 0, a^1_{kn,1}, a^1_{kn,2}, a^1_{kn,3}\right] \tag{39}$$

for the FFT implemented. The matrix elements in (39) need to be evaluated simultaneously so as to take advantage of the recursive nature of $I_{ij}(sR/c)$. Thus, the computational complexity depends almost linearly on the number of orders of the Laguerre polynomials.

2.3.3. Adaptive Stopping Criterion for TDPO Region

The first derivative of $J_k^{PO}(t)$ in terms of time t, which is given in (19), usually requires higher order polynomial expansions than that of $J_k^{PO}(t)$ to get the same accuracy [10]. Thus, we terminate the MOD formulation (20) for the TDPO region with a specified tolerance ε^{PO}, when

$$\left\|R^{PO}_{k,i}(t)\right\|_2 = \left\| \frac{d}{dt} J_k^{PO}(t) - \sum_{j=0}^{i} \left(J^{PO}_{k,j}\right)^{(1)} \phi_j(t) \right\|_2 < \varepsilon^{PO} \left\| \frac{d}{dt} J_k^{PO}(t) \right\|_2 \tag{40}$$

where $R^{PO}_{k,i}(t)$ is termed as error function. The term $\|\cdot\|_2$ refers to the 2-norm. A good approximation for $\|R^{PO}_{k,i}(t)\|_2$ and $\|(d/dt)J_k^{PO}(t)\|_2$ is needed to control the algorithm, since an exact computation of (40) requires complete knowledge of $J_k^{PO}(t)$. Therefore, a practical overall stopping criterion for the TDPO region is defined as

$$\left\{ \sum_{j=0}^{5} \sqrt{\sum_{k=1}^{N_S^{PO}} \left[\left(J^{PO}_{k,i-j}\right)^{(1)}\right]^2} \Big/ 6 \right\} \Big/ \sqrt{\sum_{j=0}^{i} \left\{ \sum_{k=1}^{N_S^{PO}} \left[\left(J^{PO}_{k,j}\right)^{(1)}\right]^2 \right\}} < \varepsilon^{PO} \tag{41}$$

where the orthogonal relations of the Laguerre polynomials are used to derive (41). The computational cost of the stopping criterion (41)

is $O\left(N_S^{PO}\right)$ for every order marched, with $O\left(N_O\right)$ memory required. Thus, when (41) is satisfied, the recursive procedure (20) stops.

If the criterion (41) is satisfied at order N_O^{PO}, the recursive procedure (20) stops, and we only need to solve a simplified version of (37) and (38), i.e.,

$$\sum_{n=1}^{N_S^{IE}} Z_{mn}^{SS} J_{n,i}^{IE} + \sum_{n=1}^{N_W^{IE}} Z_{mn}^{SW} I_{n,i}^{IE} = V_{m,i}^{E} - P_{m,i}^{IE} - P_{m,i}^{PO} \tag{42}$$

$$\sum_{n=1}^{N_S^{IE}} Z_{mn}^{WS} J_{n,i}^{IE} + \sum_{n=1}^{N_W^{IE}} Z_{mn}^{WW} I_{n,i}^{IE} = U_{m,i}^{E} - Q_{m,i}^{IE} - Q_{m,i}^{PO} \tag{43}$$

until the stopping criterion for the TDIE region is met.

2.3.4. Adaptive Stopping Criterion for TDIE Region

Similarly, the adaptive stopping criterion for the TDIE region is given by

$$\left\{ \sum_{j=0}^{5} \sqrt{\sum_{n=1}^{N_S^{IE}} \left[\left(J_{n,i-j}^{IE} \right)^{(1)} \right]^2 + \sum_{n=1}^{N_W^{IE}} \left[\left(I_{n,i-j}^{IE} \right)^{(1)} \right]^2} \Big/ 6 \right\}$$
$$\Big/ \sqrt{\sum_{j=0}^{i} \left\{ \sum_{n=1}^{N_S^{IE}} \left[\left(J_{n,j}^{IE} \right)^{(1)} \right]^2 + \sum_{n=1}^{N_W^{IE}} \left[\left(I_{n,j}^{IE} \right)^{(1)} \right]^2 \right\}} < \varepsilon^{IE} \tag{44}$$

for the given tolerance ε^{IE}. Computing (44) needs $O\left(N_S^{IE} + N_W^{IE}\right)$ CPU time and $O\left(N_O\right)$ memory storage.

If (44) is satisfied at order N_O^{IE} and (41) is not met yet, we only need to compute (20) recursively. The overall hybrid algorithm stops as both criterions (41) and (44) are satisfied.

2.3.5. Computational Cost

It is necessary to compare computational cost of the proposed hybrid method with that of conventional TDIE-MOD solver, which leads to a set of dense matrix equations. The memory required to solve the whole problem by the TDIE-MOD method [8] is $O((N_S^{IE} + N_W^{IE} + N_S^{PO})^2)$, with $O((N_S^{IE} + N_W^{IE} + N_S^{PO})^2 (N_O)^2)$ CPU time consumed.

The computational cost of the proposed method is analyzed as follows.

a) *System Matrix Construction Cost*: This cost, when the direct solution method is used, can be considered as $O((N_S^{IE} + N_W^{IE})N_S^{PO})$ for matrix fill-in and $O((N_S^{IE} + N_W^{IE})^2 N_S^{PO})$ for matrix multiplication. However, if $(N_S^{IE} + N_W^{IE}) \gg N_O$, the second cost should be avoided by using the iterative method, because it is not required to have the system matrix in an explicit form. The memory required to store the system matrix is $O((N_S^{IE} + N_W^{IE})^2)$.

b) *Right-Hand Side Computation*: The computational complexity in the construction of (20), (37) and (38) is dominated by the matrix fill-in and vector sum that appears on their right-hand side, which requires $O((N_S^{IE} + N_W^{IE})N_S^{PO}(N_O)^2)$ operation. This burden can be partially alleviated by using the FFT-based blocking scheme described in Section 2.3.2, which allows the RHS of (20), (37) and (38) to be evaluated in $O((N_S^{IE} + N_W^{IE})N_S^{PO} N_O \log^2(N_O))$ operation. The memory required to store the matrix $[\beta_{mk}^{SS}]$ and $[\beta_{mk}^{WS}]$ is $O((N_S^{IE} + N_W^{IE})N_S^{PO})$.

c) *Solution of the Linear System Equations*: The cost of inversion of the system matrix is denoted by $O((N_S^{IE} + N_W^{IE})^3)$. If an iterative method is employed to solve (37) and (38), the computational cost per order is $O(K(N_S^{IE} + N_W^{IE})N_S^{PO})$, where K is the iteration number required for convergence.

It is clear that the predominant cost of the hybrid TDIE-TDPO method is $O((N_S^{IE} + N_W^{IE})N_S^{PO} N_O \log^2(N_O))$. The relative CPU time and memory consumption with respect to the conventional TDIE-MOD [5] are represented by

$$\text{Relative CPU Time} \approx \frac{\left(N_S^{IE} + N_W^{IE}\right)\log^2(N_O)}{\left(N_S^{IE} + N_W^{IE} + N_S^{PO}\right)N_O} \tag{45}$$

$$\text{Relative Memory Cost} \approx \frac{N_S^{IE} + N_W^{IE}}{N_S^{IE} + N_W^{IE} + N_S^{PO}} \tag{46}$$

Thus, it is found that the aforementioned hybrid method can reduce the computational cost significantly when $N_S^{PO} \gg (N_S^{IE} + N_W^{IE})$.

3. NUMERICAL RESULT AND DISCUSSION

This section presents some typical numerical examples to verify the effectiveness of our proposed method. In each of them given below, we use a temporal pulse with a modulated Gaussian shape as the

excitation, and described by

$$\vec{E}_i(\vec{r},t) = -\hat{p}V_0\frac{4}{cT\sqrt{\pi}}\cos(2\pi f_0 t)\,e^{-\gamma^2} \tag{47}$$

$$\gamma = \frac{4}{cT}\left(ct - ct_0 - \vec{r}\cdot\hat{k}\right) \tag{48}$$

where f_0 is the central frequency of the pulse, $\hat{k}$ is the direction of the wave propagation, $\hat{p}$ is the polarization vector, t is the time variable, T is the pulse width, and ct_0 is the time delay.

At first, we consider a sphere centrally placed in front of a square plate, as shown in Fig. 3. Its radius is 0.1 m, the side length of the PEC square plate 3 m, and the distance between the sphere center and the plate 1 m. The polarization state of the incident field is along the direction of $\hat{y}$, and its propagation direction is $-\hat{z}$. Other parameters are chosen to be $T = 26.67$ ns, $V_0 = 2.0$ KV, and $f_0 = 200$ MHz. In particular, we set $s = 3.4 \times 10^9$.

The extent of TDIE region in our numerical experiment is the sphere, with the TDPO region on the plate. When we choose the tolerance $\varepsilon^{PO} = \varepsilon^{IE} = 0.01$, the adaptive MOD scheme stops at $N_O^{PO} = 76$ and $N_O^{IE} = 83$. Fig. 4 shows the transient current distribution across the edge 1 on the top of sphere. Fig. 5 compares the TDIE-TDPO and the TDIE-MOD solutions for the backward scattered field in the far zone. It is evident that good agreement is obtained between them. The stability performance of our hybrid solver is shown in Fig. 6. It is demonstrated that the transient currents obtained by the MOD-based TDIE-TDPO method decrease exponentially in the late-time, with no instability which may appear in some MOT-based hybrid schemes [31].

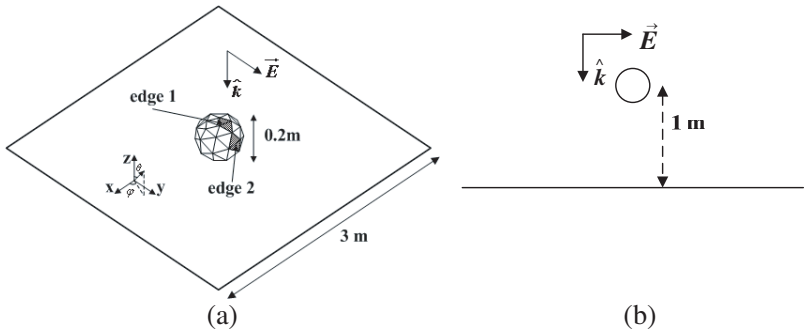

Figure 3. The arrangement of a PEC sphere and a plate. (a) Front and (b) side views.

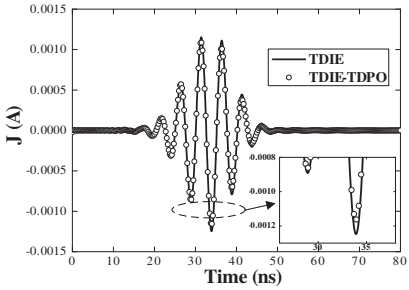

Figure 4. Comparison of the transient current across edge 1.

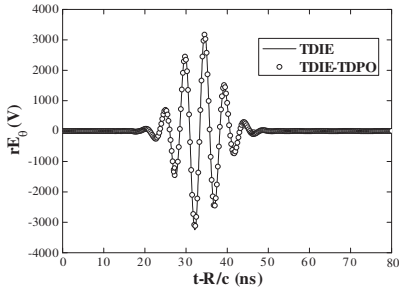

Figure 5. Comparison in the captured far field components.

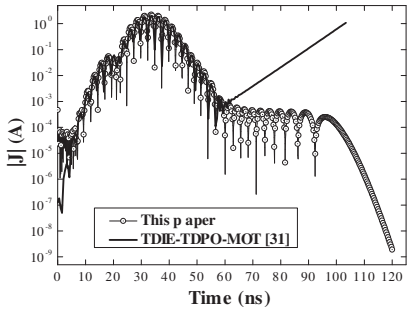

(a)

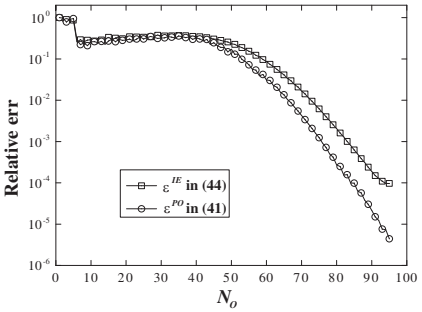

(b)

Figure 6. (a) Magnitude of the transient current distributions across Edge 2. (b) Relative error computed by (41) and (44)

Secondly, three thin wires, as shown in Fig. 7, are placed in front of a PEC cylinder. The wires are parallel to the cylinder axis with an angular separation of 3.75°. The cylinder diameter is 3 m and its height 3 m. Each wire radius is 0.5 cm, with the length of 0.5 m. They are placed at 0.5 m far from the cylinder surface. The wires are in the TDIE region and the cylinder is in the TDPO one. The parameters and waveform of the incident field are the same as those assumed before. When we choose the tolerance $\varepsilon^{PO} = \varepsilon^{IE} = 0.01$, the adaptive MOD scheme stops at $N_O^{PO} = 74$ and $N_O^{IE} = 86$.

Figure 7 shows the captured transient current distribution at location 1, with the backward scattered far field plotted in Fig. 8. An excellent agreement is observed between the results obtained by the hybrid TDIE-TDPO method and the full TDIE one. Both computational complexity and memory requirement of the TDIE-TDPO method are compared with those of conventional TDIE-MOD scheme, as shown in Figs. 9 and 10, respectively. The unknown

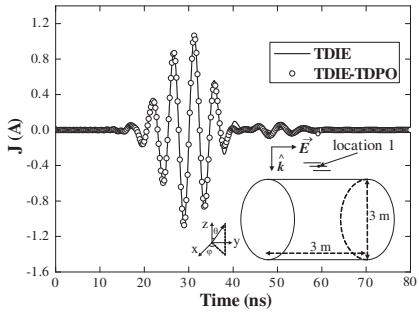

Figure 7. Comparison of the transient current at location 1.

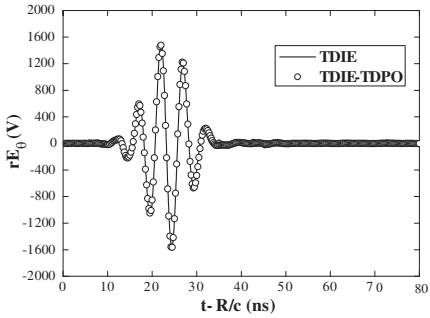

Figure 8. Comparison of the captured far field components.

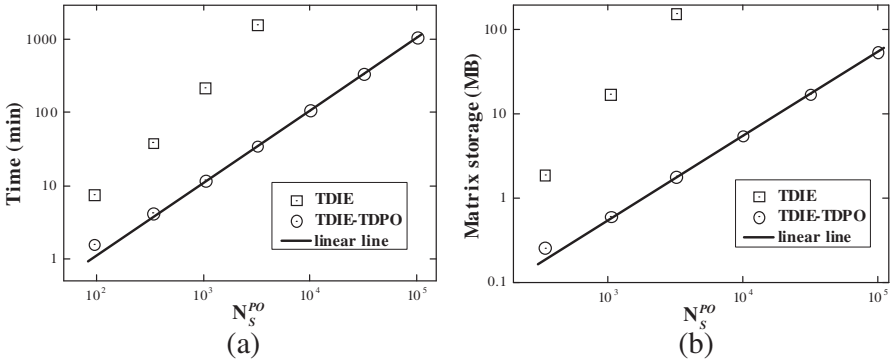

Figure 9. TDIE-TDPO versus TDIE-MOD for cylinder and wires arrangement. (a) Computational complexity. (b) Memory requirement for matrix storage.

number increases in Fig. 9 by the mesh refinement. It is indicated that the TDIE-TDPO method, as predicted in Section 2.3.5 above, always outperforms the MOD solver. It is also seen that the proposed algorithm reduces the N_O^2 dependence to $N_O \log^2(N_O)$, approximately.

Thirdly, Figs. 11(a) and (b) show the E- and H- plane radiation patterns of a parabolic reflector antenna at $f = 1.5\,\text{GHz}$, respectively, which are computed using the hybrid TDIE-TDPO method and the commercial software FEKO, respectively. The reflector is fed by a circular-dish backed dipole, and its is diameter 6.46λ with 0.375 F/D radio. $\lambda = c/f$ corresponds to the wavelength at 1.5 GHz. The circular dish of 0.553λ in diameter is situated at the location of 0.3λ far from the dipole. The wire radius of the dipole is 0.1 cm. We use the modulated Gaussian pulse (47) with $f_0 = 1.5\,\text{GHz}$, to excite the dipole. Both the dipole and circular dish are located in the TDIE region, and the reflector is in the TDPO one.

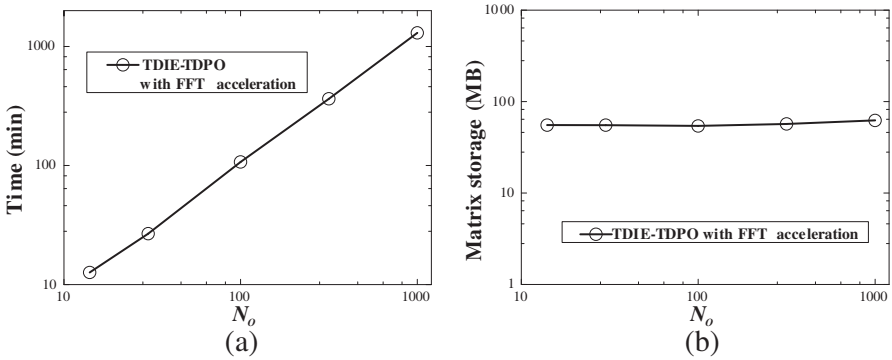

Figure 10. TDIE-TDPO for cylinder and wires arrangement, with FFT acceleration in Section 2.3.2. (a) Computational complexity with respect to $N_O^{IE} = N_O^{PO} = N_O$. (b) Memory requirement for matrix storage with respect to $N_O^{IE} = N_O^{PO} = N_O$.

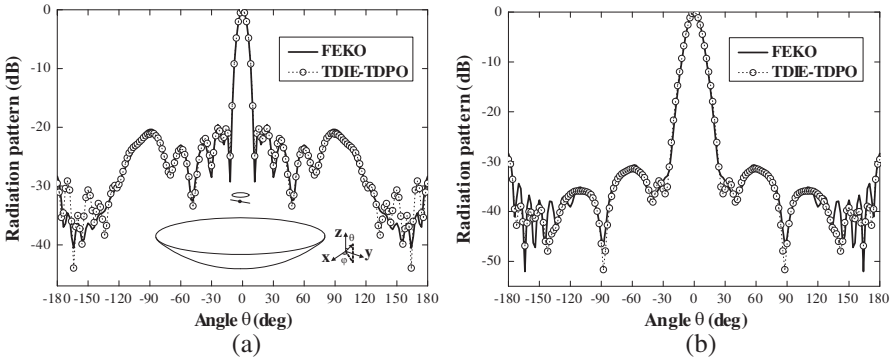

Figure 11. Radiation patterns of the parabolic reflect antenna. (a) H-plane. (b) E-plane.

It is obvious that the hybrid TDIE-TDPO results and that computed by the FEKO are in good agreement. The slight difference from $\pm 120^\circ$ to $\pm 180^\circ$ is mainly caused by edge-diffracted effects which cannot be handled using TDPO method, and partly because of the electrical size of parabolic reflector which is not large enough for minimizing the edge effects in this example. In addition, the time-domain edge diffraction could be taken into account by further hybridizing the TD-UTD [29] or TD-EEC [30], but it is beyond the scope of this work.

Finally, we consider the case of the above parabolic reflector antenna illuminated by a high-power EMP. Such an EMP can be

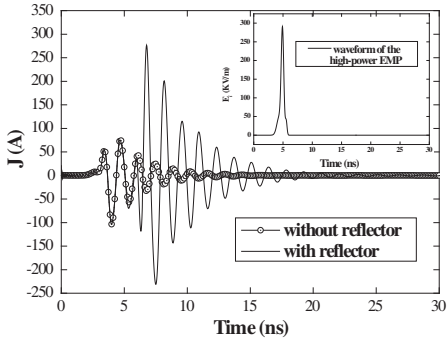

Figure 12. Transient current distribution at the feed point illuminated by a high-power EMP.

described by the curve fitting technique [9]

$$\vec{E}^i(\vec{r},t) = \hat{p}\sum_{i=1}^{3} V_i \frac{4}{cT_i\sqrt{\pi}} e^{-\gamma_i^2} \tag{49}$$

$$\gamma_i = \frac{4}{cT_i}\left(ct - ct_i - \vec{r}\cdot\hat{k}\right), \quad i = 1,2,3 \tag{50}$$

where $V_1 = 14.0\,\mathrm{KV}$, $t_1 = 4.33\,\mathrm{ns}$, $V_2 = 3.96\,\mathrm{KV}$, $t_2 = 5.54\,\mathrm{ns}$, $V_3 = 45.65\,\mathrm{KV}$, and $t_3 = 4.91\,\mathrm{ns}$. Its upper limit of frequency spectrum is up to $f_{\max} = 3\,\mathrm{GHz}$, and $\lambda_{\min} = c/f_{\max}$ corresponds to the wavelength at this frequency. When we choose the tolerance $\varepsilon^{PO} = \varepsilon^{IE} = 0.01$, the adaptive MOD scheme stops at $N_O^{PO} = 117$ and $N_O^{IE} = 90$. The dipole and circular-dish surface is solved by TDIE, and the parabolic reflector is handled with TDPO.

Figure 12 shows the comparison in transient current responses at the feed point, with and without parabolic reflector, respectively. It is shown that the magnitude of the recorded transient current on the dipole after 7 ns is strongly affected by the parabolic reflector. For example, the peak of the transient current at the feed point is about 2.7 times larger than that without the parabolic reflector, in the presence of the high-power EMP described above.

4. CONCLUSION

In this paper, a hybrid TDIE-TDPO method has been presented for solving transient electromagnetic problems with arbitrary 3-D PEC objects consisting of wires and surfaces. We have utilized an adaptive MOD method with FFT-based blocking scheme to handle

such composite problem. The above numerical results demonstrate its capability with high efficiency and accuracy. It can, in comparison with conventional TDIE-MOD method, reduce both CPU time and memory requirements significantly. Therefore, its implementation can widely extend the applicability of the marching-on-in-degree technique, and various transient electromagnetic responses of a lot of composite objects can be predicted for EMC design, EMI reduction as well as EM protection.

ACKNOWLEDGMENT

The authors acknowledge the financial support by the National Natural Science Foundation of China under Grant 60831002. Wen-Yan Yin also appreciates the support from the Sate Key Lab of Science and Technology of EMC, the Centre for Ship Development and Design, Wuhan of China.

APPENDIX A.

The variables in (29), (30), (37) and (38) are defined by

$$c^s_{mn,i-j} = \int_S \vec{f}^S_m(\vec{r}) \cdot \int'_S \frac{I_{ij}(sR/c)}{R} \vec{f}^S_n(\vec{r}')\, dS' dS \tag{A1}$$

$$c^h_{mn,i-j} = \int_S \nabla \cdot \vec{f}^S_m(\vec{r}) \cdot \int'_S \frac{I_{ij}(sR/c)}{4\pi R} \nabla' \cdot \vec{f}^S_n(\vec{r}')\, dS' dS \tag{A2}$$

$$d^s_{mn,i-j} = \int_S \vec{f}^S_m(\vec{r}) \cdot \int'_L \int_{-\pi}^{\pi} \frac{I_{ij}(sR/c)}{R} \vec{f}^W_n(\vec{r}')\, a d\varphi' dl' dS \tag{A3}$$

$$d^h_{mn,i-j} = \int_S \nabla \cdot \vec{f}^S_m(\vec{r}) \cdot \int'_L \int_{-\pi}^{\pi} \frac{I_{ij}(sR/c)}{R} \nabla' \cdot \vec{f}^W_n(\vec{r}')\, a d\varphi' dl' dS \tag{A4}$$

$$e^s_{mn,i-j} = \int_L \int_{-\pi}^{\pi} \vec{f}^W_m(\vec{r})\, a d\varphi dl \int'_S \frac{I_{ij}(sR/c)}{R} \vec{f}^S_n(\vec{r}')\, dS' \tag{A5}$$

$$e^h_{mn,i-j} = \int_L \int_{-\pi}^{\pi} \nabla' \cdot \vec{f}^W_m(\vec{r})\, a d\varphi dl \cdot \int'_S \nabla \cdot \vec{f}^S_n(\vec{r}') \frac{I_{ij}(sR/c)}{R} dS' \tag{A6}$$

$$f^s_{mn,i-j} = \int_L \int_{-\pi}^{\pi} \vec{f}^W_m(\vec{r})\, a d\varphi dl \cdot \int'_L \int_{-\pi}^{\pi} \frac{I_{ij}(sR/c)}{R} \vec{f}^W_n(\vec{r})\, a d\varphi' dl' \tag{A7}$$

$$f^h_{mn,i-j} = \int_L \int_{-\pi}^{\pi} \nabla' \cdot \vec{f}^W_m(\vec{r})\, a d\varphi dl \cdot \int'_L \int_{-\pi}^{\pi} \frac{I_{ij}(sR/c)}{R} \nabla' \cdot \vec{f}^W_n(\vec{r})\, a d\varphi' dl' \tag{A8}$$

$$\beta^{SS}_{mk} = \frac{\mu s}{8\pi} c^s_{mk,0} + \frac{1}{2\pi\varepsilon s} c^h_{mk,0}, \quad \beta^{WS}_{mk} = \frac{\mu s}{8\pi} e^s_{mk,0} + \frac{1}{2\pi\varepsilon s} e^h_{mk,0} \tag{A9}$$

$$\gamma_{kn}^{SS}=\frac{s}{8\pi c}a_{kn,0}^{1}+\frac{1}{4\pi}a_{kn,0}^{2},\quad \gamma_{kn}^{SW}=\frac{s}{8\pi c}b_{kn,0}^{1}+\frac{1}{4\pi}b_{kn,0}^{2} \tag{A10}$$

$$\begin{aligned}
Z_{mn}^{SS}&=\frac{\mu s}{8\pi}c_{mn,0}^{s}+\frac{1}{2\pi\varepsilon s}c_{mn,0}^{h}+\sum_{k=1}^{N_S^{PO}}\beta_{mk}^{SS}\gamma_{kn}^{SS},\\
Z_{mn}^{SW}&=\frac{\mu s}{8\pi}d_{mn,0}^{s}+\frac{1}{2\pi\varepsilon s}d_{mn,0}^{h}+\sum_{k=1}^{N_S^{PO}}\beta_{mk}^{SS}\gamma_{kn}^{SW}
\end{aligned} \tag{A11}$$

$$\begin{aligned}
Z_{mn}^{WS}&=\frac{\mu s}{8\pi}e_{mn,0}^{s}+\frac{1}{2\pi\varepsilon s}e_{mn,0}^{h}+\sum_{k=1}^{N_S^{PO}}\beta_{mk}^{WS}\gamma_{kn}^{SS},\\
Z_{mn}^{WW}&=\frac{\mu s}{8\pi}f_{mn,0}^{s}+\frac{1}{2\pi\varepsilon s}f_{mn,0}^{h}+\sum_{k=1}^{N_S^{PO}}\beta_{mk}^{WS}\gamma_{kn}^{SW}
\end{aligned} \tag{A12}$$

$$\begin{aligned}
P_{m,i}^{IE}=&\sum_{n=1}^{N_S^{IE}}\frac{\mu s}{4\pi}c_{mn,0}^{s}\sum_{l=0}^{i-1}J_{n,j}^{IE}+\sum_{n=1}^{N_S^{IE}}\frac{1}{\pi\varepsilon s}c_{mn,0}^{h}\sum_{l=0}^{i-1}(-1)^{i-l}\,J_{n,j}^{IE}\\
&+\sum_{n=1}^{N_W^{IE}}\frac{\mu s}{4\pi}d_{mn,0}^{s}\sum_{l=0}^{i-1}I_{n,j}^{IE}+\sum_{n=1}^{N_W^{IE}}\frac{1}{\pi\varepsilon s}d_{mn,0}^{h}\sum_{l=0}^{i-1}(-1)^{i-l}\,I_{n,j}^{IE}\\
&+\sum_{j=0}^{i-1}\sum_{n=1}^{N_S^{IE}}\frac{\mu s}{4\pi}\left(J_{n,j}^{IE}\right)^{(1)}\cdot c_{mn,i-j}^{s}+\sum_{j=0}^{i-1}\sum_{n=1}^{N_S^{IE}}\frac{1}{2\pi\varepsilon s}\left(J_{n,j}^{IE}\right)^{(-1)}\cdot c_{mn,i-j}^{h}\\
&+\sum_{j=0}^{i-1}\sum_{n=1}^{N_W^{IE}}\frac{\mu s}{4\pi}\left(I_{n,j}^{IE}\right)^{(1)}\cdot d_{mn,i-j}^{s}+\sum_{j=0}^{i-1}\sum_{n=1}^{N_W^{IE}}\frac{1}{2\pi\varepsilon s}\left(I_{n,j}^{IE}\right)^{(-1)}\cdot d_{mn,i-j}^{h}
\end{aligned} \tag{A13}$$

$$\begin{aligned}
P_{m,i}^{PO}=&\sum_{k=1}^{N_S^{PO}}\frac{\mu s}{4\pi}c_{mk,0}^{s}\sum_{l=0}^{i-1}J_{n,j}^{PO}+\sum_{k=1}^{N_S^{PO}}\frac{1}{\pi\varepsilon s}c_{mk,0}^{h}\sum_{l=0}^{i-1}(-1)^{i-l}\,J_{n,j}^{PO}\\
&+\sum_{j=0}^{i-1}\sum_{k=1}^{N_S^{PO}}\frac{\mu s}{4\pi}\left(J_{k,j}^{PO}\right)^{(1)}\cdot c_{mk,i-j}^{s}+\sum_{j=0}^{i-1}\sum_{k=1}^{N_S^{PO}}\frac{1}{2\pi\varepsilon s}\left(J_{k,j}^{PO}\right)^{(-1)}\cdot c_{mk,i-j}^{h}
\end{aligned} \tag{A14}$$

$$Q_{m,i}^{IE}=\sum_{n=1}^{N_S^{IE}}\frac{\mu s}{4\pi}e_{mn,0}^{s}\sum_{l=0}^{i-1}J_{n,j}^{IE}+\sum_{n=1}^{N_S^{IE}}\frac{1}{\pi\varepsilon s}e_{mn,0}^{h}\sum_{l=0}^{i-1}(-1)^{i-l}\,J_{n,j}^{IE}$$

$$+\sum_{n=1}^{N_W^{IE}}\frac{\mu s}{4\pi}f_{mn,0}^{s}\sum_{l=0}^{i-1}I_{n,j}^{IE}+\sum_{n=1}^{N_W^{IE}}\frac{1}{\pi\varepsilon s}f_{mn,0}^{h}\sum_{l=0}^{i-1}(-1)^{i-l}\,I_{n,j}^{IE}$$
$$+\sum_{j=0}^{i-1}\sum_{n=1}^{N_S^{IE}}\frac{\mu s}{4\pi}\left(J_{n,j}^{IE}\right)^{(1)}\cdot e_{mn,i-j}^{s}+\sum_{j=0}^{i-1}\sum_{n=1}^{N_S^{IE}}\frac{1}{2\pi\varepsilon s}\left(J_{n,j}^{IE}\right)^{(-1)}\cdot e_{mn,i-j}^{h}$$
$$+\sum_{j=0}^{i-1}\sum_{n=1}^{N_W^{IE}}\frac{\mu s}{4\pi}\left(I_{n,j}^{IE}\right)^{(1)}\cdot f_{mn,i-j}^{s}+\sum_{j=0}^{i-1}\sum_{n=1}^{N_W^{IE}}\frac{1}{2\pi\varepsilon s}\left(I_{n,j}^{IE}\right)^{(-1)}\cdot f_{mn,i-j}^{h} \quad \text{(A15)}$$

$$Q_{m,i}^{PO}=\sum_{k=1}^{N_S^{PO}}\frac{\mu s}{4\pi}e_{mk,0}^{s}\sum_{l=0}^{i-1}J_{n,j}^{PO}+\sum_{k=1}^{N_S^{PO}}\frac{1}{\pi\varepsilon s}e_{mk,0}^{h}\sum_{l=0}^{i-1}(-1)^{i-l}\,J_{n,j}^{PO}$$
$$+\sum_{j=0}^{i-1}\sum_{k=1}^{N_S^{PO}}\frac{\mu s}{4\pi}\left(J_{k,j}^{PO}\right)^{(1)}\cdot e_{mk,i-j}^{s}+\sum_{j=0}^{i-1}\sum_{k=1}^{N_S^{PO}}\frac{1}{2\pi\varepsilon s}\left(J_{k,j}^{PO}\right)^{(-1)}\cdot e_{mk,i-j}^{h} \quad \text{(A16)}$$

REFERENCES

1. Bluck, M. J. and S. P. Walker, "Time-domain BIE analysis of large three dimensional electromagnetic scattering problems," *IEEE Trans. on Antennas and Propagat.*, Vol. 45, No. 5, 894–901, May 1997.
2. Wang, X., R. A. Wildman, D. S. Weile, and P. Monk, "A finite difference delay modeling approach to the discretization of the time domain integral equations of electromagnetics," *IEEE Trans. on Antennas and Propagat.*, Vol. 56, No. 8, Part 1, 2442–2452, Aug. 2008.
3. Andriulli, F. P., K. Cools, F. Olyslager, and E. Michielssen, "Time domain Calderón identities and their application to the integral equation analysis of scattering by PEC objects part II: Stability," *IEEE Trans. on Antennas and Propagat.*, Vol. 57, No. 8, 2365–2375, Aug. 2009.
4. Zhang, G.-H., M. Xia, and X.-M. Jiang, "Transient analysis of wire structures using time domain integral equation method with exact matrix elements," *Progress In Electromagnetics Research*, Vol. 92, 281–298, 2009.
5. Jung, B. H., Y.-S. Chung, and T. K. Sarkar, "Time-domain EFIE, MFIE, and CFIE formulations using laguerre polynomials as temporal basis functions for the analysis of transient scattering

from arbitrary shaped conducting structures," *Progress In Electromagnetics Research*, Vol. 39, 1–45, 2003.

6. Ji, Z., T. K. Sarkar, B. H. Jung, Y. S. Chung, M. Salazar-Palma, and M. Yuan, "A stable solution of time domain electric field integral equation for thin-wire antennas using the Laguerre polynomials," *IEEE Trans. on Antennas and Propagat.*, Vol. 52, No. 10, 2641–2649, Oct. 2004.
7. Jung, B.-H., T. K. Sarkar, and Y.-S. Chung, "Solution of time domain PMCHW formulation for transient electromagnetic scattering from arbitrarily shaped 3-D dielectric objects," *Progress In Electromagnetics Research*, Vol. 45, 291–312, 2004.
8. Jung, B. H., Z. Ji, T. K. Sarkar, M. Salazar-Palma, and M. Yuan, "A comparison of marching-on in time method with marching-on in degree method for the TDIE solver," *Progress In Electromagnetics Research*, Vol. 70, 281–296, 2007.
9. Xue, M. F. and W. Y. Yin, "Wideband pulse responses of fractal monopole antennas under the impact of an EMP," *IEEE Trans. on Electromagn. Compat.*, Vol. 52, No. 1, 98–107, Feb. 2010.
10. Zhu, M. D., X. L. Zhou, and W. Y. Yin, "An adaptive marching-on-in-order method with FFT-based blocking scheme," *IEEE Antennas Wireless Propag. Lett.*, Vol. 9, 436–439, 2010.
11. Shanker, B., A. A. Ergin, M. Lu, and E. Michielssen, "Fast analysis of transient electromagnetic scattering phenomena using the multilevel plane wave time domain algorithm," *IEEE Trans. on Antennas and Propagat.*, Vol. 51, No. 3, 628–641, Mar. 2003.
12. Yılmaz, A. E., J. M. Jin, and E. Michielssen, "Time domain adaptive integral method for surface integral equations," *IEEE Trans. on Antennas and Propagat.*, Vol. 52, No. 10, 2692–2708, Oct. 2004.
13. Yılmaz, A. E., D. S. Weile, B. Shanker, J. M. Jin, and E. Michielssen, "Fast analysis of transient scattering in lossy media," *IEEE Antennas Wireless Propag. Lett.*, Vol. 1, 14–17, 2002.
14. Sun, E. Y. and W. V. T. Rusch, "Time-domain physical-optics," *IEEE Trans. on Antennas and Propagat.*, Vol. 42, 9–15, Jan. 1994.
15. Jakobus U. and F. M. Landstorfer, "Improved PO-MM hybrid formulation for scattering from three-dimensional perfectly conducting bodies of arbitrary shape," *IEEE Trans. on Antennas and Propagat.*, Vol. 43, No. 2, 162–169, Feb. 1995.
16. Hodges, R. E. and Y. Rahmat-Samii, "An iterative current-based hybrid method for complex structures," *IEEE Trans. on Antennas*

and Propagat., Vol. 43, 265–276, Feb. 1997.

17. Obelleiro, F., J. M. Taboada, J. L. Rodríguez, J. O. Rubiños, and A. M. Arias, "Hybrid moment-method physical-optics formulation for modeling the electromagnetic behavior of on-board antennas," *Microwave Opt. Technol. Lett.*, Vol. 27, No. 2, 88–93, Oct. 2000.
18. Djordjević, M. and B. M. Notaroš, "Higher order hybrid method of moments-physical optics modeling technique for radiation and scattering from large perfectly conducting surfaces," *IEEE Trans. on Antennas and Propagat.*, Vol. 53, No. 2, 800–813, Feb. 2005.
19. Chen, M., Y. Zhang, X. W. Zhao and C. H. Liang, "Analysis of antenna around NURBS surface with hybrid MoM-PO technique," *IEEE Trans. on Antennas and Propagat.*, Vol. 55, No. 2, 407–413, Feb. 2007.
20. Walker, S. P. and M. J. Vartiainen, "Hybridization of curvilinear time-domain integral equation and time-domain optical methods for electromagnetic scattering analysis," *IEEE Trans. on Antennas and Propagat.*, Vol. 46, No. 3, 318–324, Mar. 1998.
21. Kobidze, G., B. Shanker, and E. Michielssen, "Hybrid PO-PWTD scheme for analyzing of scattering from electrically large PEC objects," *IEEE Antennas and Propagation Society Int. Symp.*, Vol. 3, 547–555, 2003.
22. Qin, S. T., S. X. Gong, R. Wang, and L. X. Guo, "A TDIE/TDPO hybrid method for the analysis of TM transient scattering from two-dimensional combinative conducting cylinders," *Progress In Electromagn. Research*, Vol.102, 181–195, 2010.
23. Junker, G. P., A. A. Kishk, and A. W. Glisson, "A novel delta gap source model for center fed cylindrical dipoles," *IEEE Trans. on Antennas and Propagat.*, Vol. 43, No. 5, 537-540, May 1995.
24. Rao, S. M., D. R. Wilton, and A. W. Glisson, "Electromagnetic scattering by surfaces of arbitrary shape," *IEEE Trans. on Antennas and Propagat.*, Vol. 30, No. 3, 409–418, May 1982.
25. Glassner, A. S., *An Introduction to Ray Tracing*, Academic Press, 1989.
26. Rius, J. M., M. Ferrando, and L. Jofre, "High-frequency RCS of complex radar targets in real-time," *IEEE Trans. on Antennas and Propagat.*, Vol. 41, No. 9, 1308–1319, Sep. 1993.
27. Asvestas, J., "The physical-optics integral and computer graphics," *IEEE Trans. on Antennas and Propagat.*, Vol. 42, No. 12, 1459–1460, Dec. 1995.
28. Hairer, E., C. H. Lubich, and M. Schlichte, "Fast numerical solution of nonlinear Volterra convolution equations," *SIAM J.*

Sci. Stat. Comput., Vol. 6, No. 3, 532–541, 1985.

29. Veruttipong, T. W., "Time domain version of the uniform GTD," *IEEE Trans. on Antennas and Propagat.*, Vol. 38, No. 11, 1757–1764, Nov. 1990.
30. Altıntaş, A. and P. Russer, "Time-domain equivalent edge currents for transient scattering," *IEEE Trans. on Antennas and Propagat.*, Vol. 49, No. 4, 602–606, Apr. 2001.
31. Luo, W., W. Y. Yin, M. D. Zhu, and J. Y. Zhao, "Hybrid TDIE-TDPO method for studying on transient responses of some wire and surface structures illuminated by an electromagnetic pulse," *Progress In Electromagnetics Research*, Vol. 116, 203–219, 2011.
32. Luo, W., W. Y. Yin, M. D. Zhu, and J. F. Mao, "Investigation on electromagnetic responses of some complex wire-surface composite objects using hybrid TDIE-TDPO based MOT method," *IEEE Electronmagn. Compat. Symp.*, Aug. 2011, 579–584.
33. Zhu, M. D., X. L. Zhou, and W. Y. Yin, "Investigation on electromagnetic responses of double objects illuminated by a high-power EMP using hybrid TDIE-TDPO method," *IEEE Electronmagn. Compat. Symp.*, 547–555, Aug. 2010.
34. Zhu, H., Z.-H. Wu, X. Y. Zhang, and B.-J. Hu, "Time-domain integral equation solver for radiation from dipole antenna loaded with general bi-isotropic objects," *Progress In Electromagnetics Research B*, Vol. 35, 349–367, 2011.
35. Guan, Y., S.-X. Gong, S. Zhang, B. Lu, and T. Hong, "A novel time-domain physical optics for computation of electromagnetic scattering of homogeneous dielectric objects," *Progress In Electromagnetics Research M*, Vol. 14, 123–134, 2010.
36. Li, J., B. Wei, Q. He, L.-X. Guo, and D.-B. Ge, "Time-domain iterative physical optics method for analysis of EM scattering from the target half buried in rough surface: PEC case," *Progress In Electromagnetics Research*, Vol. 121, 391–408, 2011.